This article was downloaded by: [Institute Of Atmospheric Physics]
On: 09 December 2014, At: 15:31
Publisher: Taylor & Francis
Informa Ltd Registered in England and Wales Registered Number: 1072954 Registered office: Mortimer House, 37-41 Mortimer Street, London W1T 3JH, UK

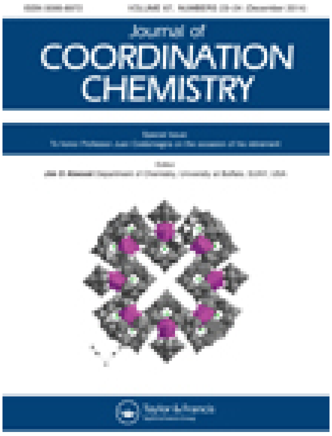

Click for updates

Journal of Coordination Chemistry
Publication details, including instructions for authors and subscription information:
http://www.tandfonline.com/loi/gcoo20

A family of hexanuclear Mn(III) single-molecule magnets

Alexandros Perivolaris[a], Athena M. Fidelli[a], Ross Inglis[b], Vadim G. Kessler[c], Alexandra M.Z. Slawin[d], Euan K. Brechin[b] & Giannis S. Papaefstathiou[a]

[a] Laboratory of Inorganic Chemistry, Department of Chemistry, National and Kapodistrian University of Athens, Zografou, Greece
[b] EaStCHEM School of Chemistry, The University of Edinburgh, Edinburgh, UK
[c] Department of Chemistry, Swedish University of Agricultural Sciences, Uppsala, Sweden
[d] School of Chemistry, The University of St. Andrews, St. Andrews, UK

Accepted author version posted online: 08 Oct 2014.Published online: 31 Oct 2014.

To cite this article: Alexandros Perivolaris, Athena M. Fidelli, Ross Inglis, Vadim G. Kessler, Alexandra M.Z. Slawin, Euan K. Brechin & Giannis S. Papaefstathiou (2014) A family of hexanuclear Mn(III) single-molecule magnets, Journal of Coordination Chemistry, 67:23-24, 3972-3986, DOI: 10.1080/00958972.2014.974583

To link to this article: http://dx.doi.org/10.1080/00958972.2014.974583

PLEASE SCROLL DOWN FOR ARTICLE

Taylor & Francis makes every effort to ensure the accuracy of all the information (the “Content”) contained in the publications on our platform. However, Taylor & Francis, our agents, and our licensors make no representations or warranties whatsoever as to the accuracy, completeness, or suitability for any purpose of the Content. Any opinions and views expressed in this publication are the opinions and views of the authors, and are not the views of or endorsed by Taylor & Francis. The accuracy of the Content should not be relied upon and should be independently verified with primary sources of information. Taylor and Francis shall not be liable for any losses, actions, claims, proceedings, demands, costs, expenses, damages, and other liabilities whatsoever or howsoever caused arising directly or indirectly in connection with, in relation to or arising out of the use of the Content.

Journal of Coordination Chemistry, 2014
Vol. 67, Nos. 23–24, 3972–3986, http://dx.doi.org/10.1080/00958972.2014.974583

A family of hexanuclear Mn(III) single-molecule magnets

ALEXANDROS PERIVOLARIS†, ATHENA M. FIDELLI†, ROSS INGLIS‡,
VADIM G. KESSLER§, ALEXANDRA M.Z. SLAWIN¶, EUAN K. BRECHIN*‡ and
GIANNIS S. PAPAEFSTATHIOU*†

†Laboratory of Inorganic Chemistry, Department of Chemistry, National and Kapodistrian University of Athens, Zografou, Greece
‡EaStCHEM School of Chemistry, The University of Edinburgh, Edinburgh, UK
§Department of Chemistry, Swedish University of Agricultural Sciences, Uppsala, Sweden
¶School of Chemistry, The University of St. Andrews, St. Andrews, UK

(*Received 16 September 2014; accepted 19 September 2014*)

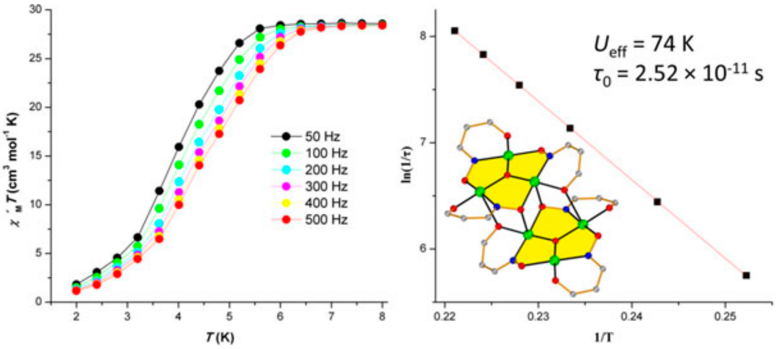

In an attempt to employ salicylic acid (HOsalH), 2,6-dihydroxy benzoic acid $\{(HO)_2PhCO_2H\}$, and naphthalene-1,8-dicarboxylic acid $\{1,8\text{-naph}(CO_2H)_2\}$ in Mn(III) salicylaldoximate chemistry as a means to alter the structural identity of the hexanucluear clusters usually obtained from this reaction system, we have isolated a family of hexanuclear Mn(III) complexes based on salicyladloxime ($saoH_2$) and 2-hydroxy-1-naphthaldehyde oxime ($naphthsaoH_2$). Five hexanuclear clusters, $[Mn_6O_2(sao)_6(HOsal)_2(EtOH)_4]\cdot EtOH$ (**1**·EtOH), $[Mn_6O_2(sao)_6\{1,8\text{-naph}(CO_2Me)(CO_2)\}_2(MeOH)_6]\cdot 3MeOH$ (**2**·3MeOH), $[Mn_6O_2(naphthsao)_6\{1,8\text{-naph}(CO_2Et)(CO_2)\}_2(EtOH)_6]$ (**3**·2MeOH), $[Mn_6O_2(naphthsao)_6(MeCO_2)_2(EtOH)_4]\cdot 2H_2O$ (**4**·2H$_2$O), and $[Mn_6O_2(naphthsao)_6\{(HO)_2PhCO_2\}_2(EtOH)_4]\cdot 4EtOH$ (**5**·4EtOH), have been synthesized and characterized by single-crystal X-ray crystallography. The magnetic properties of **3**, **4**, and **5** are discussed.

Keywords: Crystal structures; Magnetic properties; Mn(III) complexes; Oximato complexes; Single-molecule magnets

---

*Corresponding authors. Email: ebrechin@staffmail.ed.ac.uk (E.K. Brechin); gspapaef@chem.uoa.gr (G.S. Papaefstathiou)
Dedicated to Professor Juan Costamagna on the occasion of his retirement.

1. Introduction

Since the discovery of the first hexanuclear complexes of general formula $[M^{III}_6O_2(\text{-}sao)_6(O_2CR)_2(H_2O)_2(RCN)_2]$ (M = V, Cr, Mn, and Fe; R = $C(Ph)_3$, $C(Me)_3$, CH_2Ph Ph and CH_2CH_3); $saoH_2$ = salicylaldoxime) [1], manganese salicylaldoximate chemistry has been dominated by the chemistry and physics of hexanuclear and trinuclear Mn(III) clusters of formulae $[Mn^{III}_6O_2(Rsao)_6(O_2CR)_2(L)_{4–6}]$ [1–29] and $[Mn^{III}_3O(Rsao)_3(O_2CR)(L)_3]$ [30–43] (R = H, Me, Et, etc.; L = solvent), the latter being the analogous "half" molecules of the former. Several members of the $[Mn_6]$ and $[Mn_3]$ families have been found to behave as single-molecule magnets (SMMs), exhibiting slow relaxation of the magnetization. It has also been found that in each case, it was possible to significantly increase the ground spin state from $S = 4$ to $S = 12$ in the former and from $S = 2$ to $S = 6$ in the latter, by utilizing derivatized versions of the oxime ligand to distort the Mn–O–N–Mn superexchange pathway, inducing orbital orthogonality, enhancing the effective energy barrier for magnetization reversal to record levels for transition metal-based SMMs [5–8].

The ease of synthesis of $[Mn_3]$ and $[Mn_6]$ and their relative solution stability have enabled them to be utilized as starting materials – building blocks for construction of a host of discrete and infinite supramolecular architectures [14, 21, 31, 37, 41, 44–57]. The employment of auxiliary pyridyl-type ligands into the reaction mixtures of $[Mn_{3/6}]$ or in solutions of preformed $[Mn_{3/6}]$ has yielded several discrete (i.e. polygons and inter-digitated tripodal assemblies enclathrating anions) and polymeric (i.e. 1-D and 2-D coordination polymers) species featuring unique types of entanglement [37, 48], while the use of polycarboxylate ligands has driven the formation of 1-D and 2-D coordination polymers (or metal-organic frameworks) based on $[Mn_6]$ SMMs [21, 45, 46, 52, 55, 58]. Several single-chain magnets (or in some cases chains of non-interacting SMMs) consisting of $[Mn_{3/6}]$ clusters have also been reported [47, 50, 51, 54, 57].

Table 1. Manganese salicylaldoximate clusters other than the usual $[Mn_{3/6}]$.

Formula[a]	$[Mn_3(\mu\text{-}O)(Rsao)_3]^+$	S_T	SMM	U_{eff}/K	Ref.
$[Mn^{III}_4(Mesao)_4(MesaoH)_4]$	No	8	Yes	N/A	[59]
$[Mn^{III}_4(Etsao)_4(EtsaoH)_4]$	No	8	Yes	N/A	[59b]
$[Mn^{III}_4(Naphthsao)_4(NaphthsaoH)_4]$	No	8	Yes	N/A	[59b]
$[Mn^{III}_4(sao)_4(saoH)_4]$	No	–	No	–	[60]
$[Mn^{III}_3Mn^{IV}_2O_2(Etsao)_6(MeO)(Val)]$	No	2	No	–	[33, 38]
$[NEt_4]_3[Mn^{III}_3Mn^{II}_2O(sao)_3(N_3)_6Br_2]$	Yes	11	Yes	36.4	[61]
$[NEt_4]_3[Mn^{III}_3Mn^{II}_2O(Mesao)_3(N_3)_6Cl_2]$	Yes	6	Yes	39.4	[61]
$[NEt_4]_3[Mn^{III}_3Mn^{II}_2O(sao)_3(OCN)_6Cl_2]$	Yes	1	Yes	33.9	[61]
$[Mn^{III}_4Mn^{IV}_2O_2(Etsao)_6(MeO)_4(MeOH)_2]$	No	6 ± 1	No	–	[10]
$(NH_4)_2[Mn^{III}_6Mn^{II}O_2(Etsao)_6(O_2CMe)_6]$	Yes	11/2	Yes	32	[62]
$[Mn^{III}_6Mn^{II}_2O_2(Mesao)_6(N_3)_6(MeOH)_8]$	Yes	7	Yes	40	[36, 63]
$[\ Mn^{III}_6Mn^{II}_2O_2(Naphthsao)_6(N_3)_6(MeOH)_8]$	Yes	1	No	–	[36, 63]
$[Mn^{III}_9O_4(Mesao)_6(MeO)_4(O_2CMe)_3(H_2O)_2]$	Yes	6	Yes	30	[64]
$[Mn^{III}_9O_4(Mesao)_6(MeO)_3(O_2CMe)_3(OH)(MeOH)_2]$	Yes	6	Yes	35.2	[65]
$[Mn^{III}_9O_4(Menaphthsao)_6(MeO)_3(O_2CMe)_4(MeOH)_x(H_2O)_y]$	Yes	6	Yes	67	[66]
$[Mn^{III}_{12}O_4(sao)_{12}(N_3)_4(MeOH)_4(H_2O)_2]$	Yes	4	Yes	70	[67]
$[Mn^{III}_{12}O_4(sao)_{12}(N_3)_4(MeOH)_6(H_2O)_2]$	Yes	4	Yes	70	[68]
$[Mn^{III}_4Mn^{II}_8(sao)_{12}(CH_3O)_4(CH_3OH)_{12}]$	No	2	No	–	[69]
$[Mn^{III}_{14}Mn^{II}_{18}(O)_8(OH)_6(Mesao)_{14}(O_2CMe)_{18}Br_8(H_2O)_{10}]$	No	11,12	Yes	44.5	[70]

[a]Val = dl-Valine; $EtsaoH_2$ = 2-hydroxypropiophenone oxime; $MesaoH_2$ = 2-hydroxyacetophenone oxime; $saoH_2$ = salicyloaldoxime; $NaphthsaoH_2$ = 2-hydroxy-1-napthaldoxime; $MenaphthsaoH_2$ = 1-(1-hydroxynaphthalen-2-yl)ethan-1-one oxime.

Nevertheless, the increased effort for the exploitation of the manganese salicylaldoximate reaction system has also yielded several clusters with different nuclearities and metal topologies than the usual $[Mn_{3/6}]$ systems. These efforts include the addition of "extra" ingredients/ligands within the manganese salicylaldoximate reaction mixtures, which can act either as co-ligands or compete/dominate the $Rsao^{2-}$ coordination, or, in some cases, can enforce changes in the self-assembly process by their mere presence in the reaction mixture without being incorporated into the structure of the final product. These clusters are summarized in table 1 where we see that several contain the usual $[Mn_3(\mu_3\text{-}O)(Rsao)_3]^+$ moiety, with others adopting completely different metal topologies. We note that most of these clusters are SMMs.

Herein, we present results from our efforts to intentionally disturb the $[Mn_{3/6}]$ cores of the manganese salicylaldoximate clusters by incorporating into the reaction mixtures carboxylate ligands that could potentially chelate manganese ions, thus disturbing/altering the usual $[Mn_{3/6}]$ topology. For this purpose, we utilized as "extra" ingredients, 2-hydroxy benzoic acid (HOsalH, salicylic acid), 2,6-dihydroxy benzoic acid $\{(HO)_2PhCO_2H\}$, and naphthalene-1,8-dicarboxylic acid anhydride $\{1,8\text{-naph}(C_2O_3)\}$, which upon hydrolysis yields naphthalene-1,8-dicarboxylic acid $\{1,8\text{-naph}(CO_2H)_2\}$ (scheme 1). Despite our efforts, we isolated a family of $[Mn_6]$ clusters, $[Mn_6O_2(sao)_6(HOsal)_2(EtOH)_4]\cdot EtOH$ (**1**·EtOH), $[Mn_6O_2(sao)_6\{1,8\text{-naph}(CO_2Me)(CO_2)\}_2(MeOH)_6]\cdot 3MeOH$ (**2**·3MeOH), $[Mn_6O_2(naphthsao)_6\{1,8\text{-naph}(CO_2Et)(CO_2)\}_2(EtOH)_6]\cdot 2MeOH$ (**3**·2MeOH), $[Mn_6O_2(naphthsao)_6(MeCO_2)_2(EtOH)_4]\cdot 2H_2O$ (**4**·$2H_2O$), and $[Mn_6O_2(naphthsao)_6\{(HO)_2PhCO_2\}_2(EtOH)_4]\cdot 4EtOH$ (**5**·4EtOH), that adopt the usual $[Mn_6(\mu_3\text{-}O)_2(Rsao)_6]^{2+}$ core, stabilized by the monoanion of the salicylic acid ($HOsal^-$), the monoanion of the 8-(methoxycarbonyl)-1-naphthoic acid $\{1,8\text{-naph}(CO_2Me)(CO_2^-)\}$, the monoanion of the 8-(ethoxycarbonyl)-1-naphthoic acid $\{1,8\text{-naph}(CO_2Et)(CO_2^-)\}$, acetate ($MeCO_2^-$), and the monoanion of the 2,6-dihydroxy benzoic acid $\{(HO)_2PhCO_2^-\}$, respectively. The magnetic properties of **3–5** are discussed; **1** and **2** contain two different $[Mn_6]$ molecules in their asymmetric units and thus were not measured.

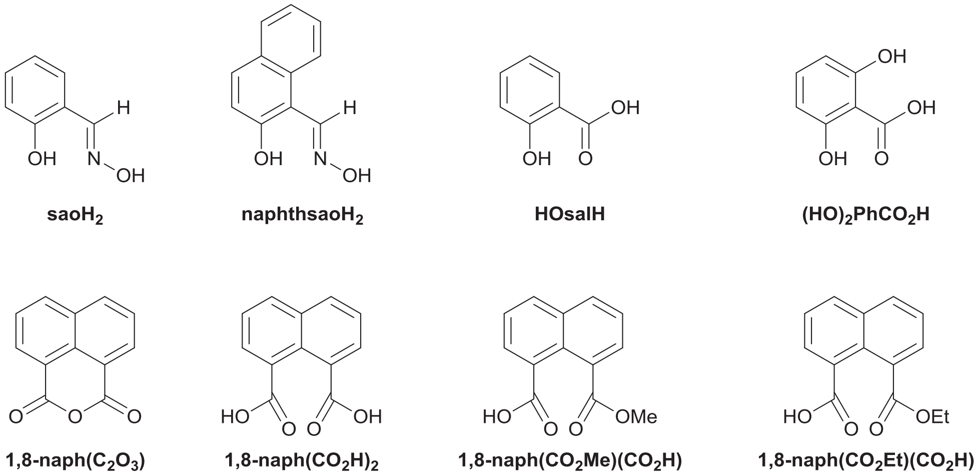

Scheme 1. Ligands discussed in the text.

2. Experimental

2.1. *General and physical measurements*

All manipulations were performed under aerobic conditions using materials as received. CAUTION! Although no problems were encountered in this work, care should be taken when using the potentially explosive perchlorate anion. Substituted salicylaldoximes were synthesized following known procedures [71]. Variable temperature, solid-state direct current (DC) down to 5 K and alternating current (AC) in the 2–8 K range, magnetic susceptibility and magnetization data in the ranges 0.5–7 T and 2–7 K were collected on a Quantum Design MPMS-XL SQUID magnetometer equipped with a 7 T DC magnet. Diamagnetic corrections were applied to the observed paramagnetic susceptibilities using Pascal's constants. Microanalyses (C, H, and N) were performed with an EA 1108 Carlo Erba analyzer. IR spectra were recorded on a Shimadzu FT/IR IRAffinity-1 spectrometer with samples prepared as KBr pellets.

2.2. *Compound preparation*

2.2.1. Synthesis of $[Mn_6O_2(sao)_6(HOsal)_2(EtOH)_4]\cdot EtOH$ (1·EtOH). $Mn(AcO)_2\cdot 4H_2O$ (98 mg, 0.4 mM), $saoH_2$ (55 mg, 0.4 mM), and $LiOH\cdot H_2O$ (16.5 mg, 0.4 mM) were stirred in 25 mL of EtOH for 30 min to afford a dark green solution. Solid HOsalH (55 mg, 0.4 mM) was added and the solution was stirred for one more hour. After filtration, the solution was left to evaporate for 4 days to afford dark green X-ray quality crystals of **1**·EtOH. The crystals were isolated by vacuum filtration, washed with Et_2O (2 × 5 mL), and dried under vacuum for several days. Yield 42% (based on Mn). Anal. Calcd for $[Mn_6O_2(sao)_6(HOsal)_2(EtOH)_4]$ ($C_{64}H_{64}Mn_6N_6O_{24}$): C, 47.13; H, 3.96; N, and 5.15. Found: C, 47.21; H, 4.01; N, and 5.17. IR (KBr pellets, cm^{-1}): 1693 m, 1616 w, 1591 sh, 1581 sh, 1536 m, 1467 w, 1455 w, 1436 s, 1378 m, 1322 w, 1282 s, 1247 w, 1197 w, 1154 w, 1121 w, 1041 sh, 1025 sh, 915 sh, 859 w, 822 w, 804 w, 755 s, 678 s, 649 m, and 554 wbr.

2.2.2. Synthesis of $[Mn_6O_2(sao)_6\{1,8\text{-naph}(CO_2Me)(CO_2)\}_2(MeOH)_6]\cdot 3MeOH$ (2·3MeOH). $Mn(ClO_4)_2\cdot 6H_2O$ (144.7 mg, 0.4 mM) and $saoH_2$ (55 mg, 0.4 mM) were stirred in 15 mL of MeOH for 10 min to afford a colorless solution. To this solution, 10 mL of an orange methanolic solution of 1,8-naph(C_2O_3) (79 mg, 0.4 mM) and $LiOH\cdot H_2O$ (33 mg, 0.8 mM) were added to afford a dark green solution. This solution was stirred for 30 min, filtered, and left to stand for 4 days to afford dark green X-ray quality crystals of **2**·3MeOH. The crystals were isolated by vacuum filtration, washed with Et_2O (2 × 5 mL), and dried under vacuum for several days. Yield 48% (based on Mn). Anal. Calcd for $[Mn_6O_2(sao)_6\{1,8\text{-naph}(CO_2Me)(CO_2)\}_2(MeOH)_6]$ ($C_{74}H_{72}Mn_6N_6O_{28}$): C, 48.75; H, 3.98; and N, 4.61. Found: C, 48.82; H, 3.90; and N, 4.58. IR (KBr pellets, cm^{-1}): 1679 m, 1593 s, 1579 m, 1540 m, 1536 m, 1469 m, 1437 s, 1410 w, 1357 w, 1326 w, 1284 sh, 1200 m, 1147 w, 1121 w, 1044 s, 1026 s, 917 sh, 754 w, 749 w, 731 w, 680 s, 650 m, 418 w, and 405 w.

2.2.3. Synthesis of $[Mn_6O_2(naphthsao)_6\{1,8\text{-naph}(CO_2Et)(CO_2)\}_2(EtOH)_6]\cdot 2MeOH$ (3·2MeOH). $Mn(ClO_4)_2\cdot 6H_2O$ (144.7 mg, 0.4 mM) and naphthsaoH_2 (75 mg, 0.4 mM) were stirred in 20 mL of EtOH for 10 min to form a colorless solution. To this solution, 15 mL of an orange methanolic solution of 1,8-naph(C_2O_3) (79 mg, 0.4 mM) and LiOH·H_2O (33 mg, 0.8 mM) were added to afford a dark green solution. This solution was stirred for 30 min, filtered, and left to stand for 4 days to afford dark green X-ray quality crystals of **3**·2MeOH. The crystals were isolated by vacuum filtration, washed with Et_2O (2 × 5 mL), and dried under vacuum for several days. Yield 50% (based on Mn). Anal. Calcd for [Mn_6O_2(naphthsao)$_6${1,8-naph(CO_2Et)(CO_2)}$_2$(EtOH)$_6$] ($C_{106}H_{100}Mn_6N_6O_{28}$): C, 56.95; H, 4.51; and N, 3.76. Found: C, 57.00; H, 4.42; and N, 3.78. IR (KBr pellets, cm^{-1}): 1708 w, 1694 wsh, 1689 w, 1647 w, 1610 sh, 1589 sh, 1570 w, 1525 s, 1502 m, 1448 w, 1423 sh, 1397 w, 1377 w, 1350 w, 1325 m, 1289 m, 1242 w, 1187 m, 1160 w, 1142 w, 1089 w, 1047 s, 1027 m, 957 s, 820 m, 789 w, 774 w, 745 w, 663 s, 576 wbr, and 517 w.

2.2.4. Synthesis of [Mn_6O_2(naphthsao)$_6$($MeCO_2$)$_2$(EtOH)$_4$]·$2H_2O$ (4·$2H_2O$). Mn (AcO)$_2$·$4H_2O$ (98 mg, 0.4 mM), naphthsaoH_2 (75 mg, 0.4 mM), and HOsalH (55 mg, 0.4 mM) were stirred in 25 mL of EtOH for 1 h and the solution became dark green. Et_3N 1 M in EtOH (0.4 mL, 0.4 mM) was added and the solution was stirred for one more hour, filtered, and left to stand for 4 days to afford dark green X-ray quality crystals of **4**·$2H_2O$. The crystals were isolated by vacuum filtration, washed with Et_2O (2 × 5 mL), and dried under vacuum for several days. Yield 47% (based on Mn). Anal. Calcd for [Mn_6O_2(naphthsao)$_6$($MeCO_2$)$_2$(EtOH)$_4$] ($C_{78}H_{72}Mn_6N_6O_{22}$): C, 52.78; H, 4.09; and N, 4.73. Found: C, 52.82; H, 3.99; and N, 4.78. IR (KBr pellets, cm^{-1}): 1613 sh, 1588 sh, 1568 m, 1528 s, 1506 w, 1450 m, 1421 s, 1380 m, 1325 s, 1288 s, 1243 m, 1187 m, 1141 w, 1090 w, 1045 s, 1026 s, 955 s, 818 m, 794 w, 765 w, 739 w, 666 sh, 519 w, 495 w, and 419 w.

2.2.5. Synthesis of [Mn_6O_2(naphthsao)$_6${$(HO)_2PhCO_2$}$_2$(EtOH)$_4$]·4EtOH (5·4EtOH). Mn(NO_3)$_2$·$4H_2O$ (100 mg, 0.4 mM), napthsaoH_2 (75 mg, 0.4 mM), and LiOH·H_2O (33 mg, 0.8 mM) were stirred in 25 mL of EtOH for 1 h during which the solution became dark green. Solid $(HO)_2PhCO_2H$ was added and the solution was further stirred for 30 min, filtered and left to stand for 5 days to afford dark green X-ray quality crystals of **5**·4EtOH. The crystals were isolated by vacuum filtration, washed with Et_2O (2 × 5 mL), and dried under vacuum for several days. Yield 50% (based on Mn). Anal. Calcd for [Mn_6O_2(naphthsao)$_6${$(HO)_2PhCO_2$}$_2$(EtOH)$_4$] ($C_{88}H_{76}Mn_6N_6O_{26}$): C, 53.84; H, 3.90; and N, 4.28. Found: C, 53.98; H, 3.81; and N, 4.35. IR (KBr pellets, cm^{-1}): 1690 w, 1635 s, 1611 sh, 1587 s, 1574 s, 1527 s, 1503 m, 1446 m, 1423 sh, 1389 s, 1326 s, 1289 s, 1244 sh, 1219 m, 1188 sh, 1159 w, 1143 w, 1091 w, 1051 s, 1028 sh, 956 s, 884 w, 824 s, 791 w, 765 w, 745 w, 664 s, 598 w, 530 w, 521 w, 499 w, 456 w, and 424 w.

2.3. *Single-crystal X-ray crystallography*

The data collection for the single crystals of the compounds were carried out at −180 °C (for **1–3**), −100 °C (for **4**), and at room temperature (for **5**) using Mo Kα radiation ($\lambda = 0.71073$ Å) for **1–3** and **5** and Cu Kα radiation ($\lambda = 1.54187$ Å) for **1** on a Rigaku Saturn70 diffractometer (for **1–4**) and on a Bruker SMART Apex-II diffractometer (for **5**). Complete crystal data and parameters for data collection and processing are reported in table 2. The structures were solved by direct methods using SIR2004 [72] (for **1**, **3**, and **4**), SIR97 [73] (for **2**), and SHELXS-97 [74] (for **5**), and refined by full-matrix least-squares techniques on F^2 with SHELXL-97 [75].

Table 2. Crystal and structure refinement data for **1–5**.

Compound reference	**1**	**2**	**3**	**4**	**5**
Chemical formula	$C_{66}H_{70}Mn_6N_6O_{25}$	$C_{77}H_{84}Mn_6N_6O_{31}$	$C_{108}H_{108}Mn_6N_6O_{30}$	$C_{78}H_{76}Mn_6N_6O_{24}$	$C_{96}H_{98}Mn_6N_6O_{30}$
Formula mass	1676.93	1919.16	2299.69	1811.11	2145.44
Crystal system	Triclinic	Triclinic	Monoclinic	Triclinic	Rhombohedral
a/Å	12.988(4)	16.0385(17)	14.750(4)	10.862(5)	21.172(6)
b/Å	14.874(6)	16.6938(18)	15.144(5)	12.495(5)	21.172(6)
c/Å	19.692(7)	16.7381(19)	31.059(10)	15.144(5)	21.172(6)
α/°	87.677(18)	76.311(6)	90.0000	93.076(4)	90.151(4)
β/°	71.746(10)	75.893(6)	93.917(5)	98.284(12)	90.151(4)
γ/°	83.064(16)	71.971(6)	90.0000	111.102(12)	90.151(4)
Unit cell volume/Å^3	3586(2)	4069.3(8)	6922(4)	1885.0(13)	9490(4)
Temperature/K	93	93	93	173	296(2)
Space group	P-1	P-1	$P2/n$	P-1	R-3
No. of formula units per unit cell, Z	2	2	2	1	3
Radiation type	Mo Kα	Mo Kα	Mo Kα	Cu Kα	Mo Kα
Absorption coefficient, μ/mm^{-1}	1.107	0.992	0.593	8.658	0.644
No. of reflections measured	36,914	40,008	68,289	24,805	19,569
No. of independent reflections	13,088	14,751	12,720	6367	9063
R_{int}	0.0937	0.0693	0.2466	0.1655	0.2262
Final R_1 values ($I > 2\sigma(I)$)	0.0951	0.0682	0.1269	0.0777	0.0910
Final R_1 values (all data)	0.1073	0.0773	0.1373	0.1213	0.1609
Final $wR(F^2)$ values (all data)	0.2737	0.2162	0.3940	0.2224	0.2843
Goodness of fit on F^2	1.130	1.093	1.619	1.048	1.088
CCDC	1024008	1024009	1024010	1024011	1024012

3. Results and discussion

3.1. *Brief synthetic comments*

Complexes **1–5** were prepared by reaction of an alcoholic solution of $saoH_2$ or $naphthsaoH_2$ with an appropriate Mn(II) salt in the presence of the corresponding auxiliary carboxylic acid (salicylic acid or 2,6-dihydroxy salicylic acid) or the anhydride of naphthalene-1,8-dicarboxylic acid. Upon addition of a base (Et_3N or $LiOH{\cdot}H_2O$) the Mn(II) is readily aerially oxidized to Mn(III) and the corresponding [Mn_6] precipitates in the form of well-shaped dark green single crystals after several days in moderate–good yields. Since we did not manage to change the identity of the [Mn_6] clusters, we attempted to add an excess of the corresponding base. In some of these experiments, we isolated the known [$Mn^{III}_4Mn^{IV}_2O_2(Rsao)_6(RO)_4(ROH)_2$] [10] as confirmed by IR spectroscopy and, in some cases, by single-crystal X-ray crystallography.

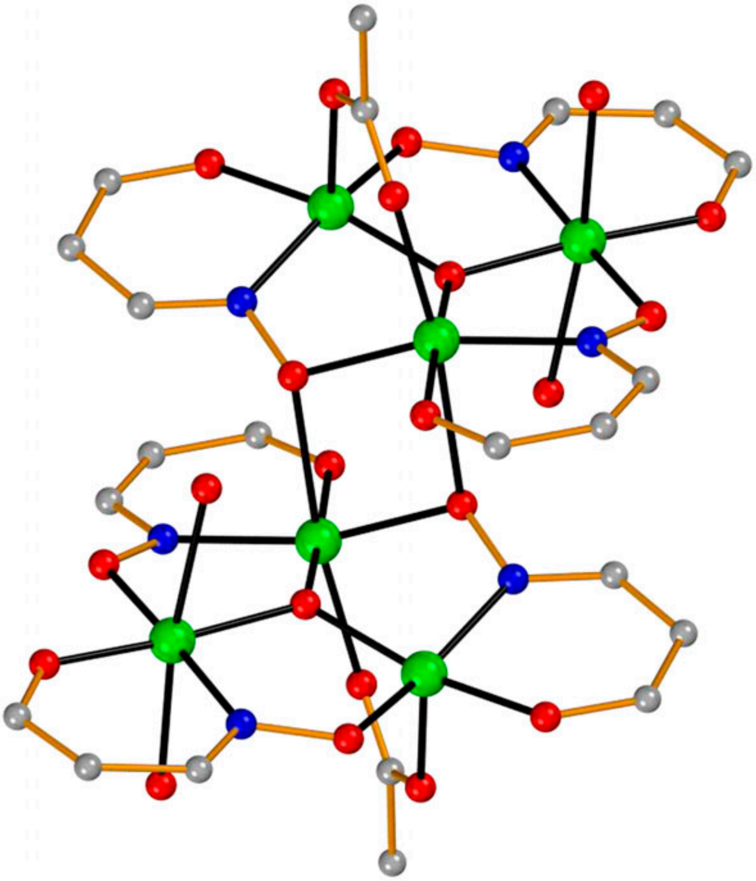

Figure 1. The [$Mn^{III}_6(\mu_3\text{-}O)_2(\mu_3\text{-}Rsao)_2(\mu_2\text{-}Rsao)_4(\mu_2\text{-}RCO_2)_2(ROH)_4$] core found in **1**, **4**, and **5**. All hydrogens and several carbons and oxygens have been removed for clarity. Color code: Mn green, O red, N blue, C gray (see http://dx.doi.org/10.1080/00958972.2014.974583 for color version).

3.2. Description of structures

Complexes **1**, **2**, and **4** crystallize in the triclinic space group *P*-1, **3** in the monoclinic space group *P2/n,* and **5** in the rhombohedral space group *R*-3. Complexes **1–5** display similar molecular structures, and therefore a general description of all crystal structures will follow, emphasizing the similarities and differences between them. The unit cells of **1** and **2** comprise two crystallographically independent $[Mn_6]$ cages ($[Mn_6]_A$ and $[Mn_6]_B$) albeit being structurally similar in their coordination geometries (i.e. possesses the same coordination modes of the ligands and the same coordination environments around Mn^{III}). The main building blocks in all complexes are two oxo-centered $[Mn^{III}_3(\mu_3\text{-O})]^{7+}$ triangular units linked via two oximate oxygens from two $\eta^1 : \eta^1 : \eta^2 : \mu_3\text{-Rsao}^{2-}$ ligands (in **1**, **2**, **4**, and **5**) or two oximate oxygens from two $\eta^1 : \eta^1 : \eta^2 : \mu_3$ Rsao^{2-} ligands, and two phenolate oxygens from two $\eta^2 : \eta^1 : \eta^1 : \mu_3\text{-Rsao}^{2-}$ ligands (in **3**). The peripheral ligation around the $[Mn^{III}_3(\mu_3\text{-O})]^{7+}$ units is completed by two or one $\eta^1 : \eta^1 : \eta^1 : \mu_2$ Rsao^{2-} ligands in **1**, **2**, **4**, **5**, and **3**, respectively. Therefore, two distinct cores, $[Mn^{III}_6(\mu_3\text{-O})_2(\mu_3\text{-Rsao})_2(\mu_2\text{-Rsao})_4]^{2+}$ and $[Mn^{III}_6(\mu_3\text{-O})_2(\mu_3\text{-Rsao})_4(\mu_2\text{-Rsao})_2]^{2+}$, are found in **1**, **2**, **4**, **5**, and **3**, respectively. Complexes **1**, **2**, **4**, and **5** comprise four Mn^{III} ions in axially elongated distorted octahedral environments and two Mn^{III} ions in axially elongated distorted square-pyramidal environments, while in **3** all Mn^{III} ions are in axially elongated distorted octahedral environments. Two capping *syn,syn* $\eta^1 : \eta^1 : \mu_2$ carboxylates and four terminal alcohol molecules (MeOH or EtOH) complete the coordination spheres around Mn^{III} in **1**, **4**, and **5**, while the coordination environment around Mn^{III} in **2** and **3** is completed by two terminal carboxylates and

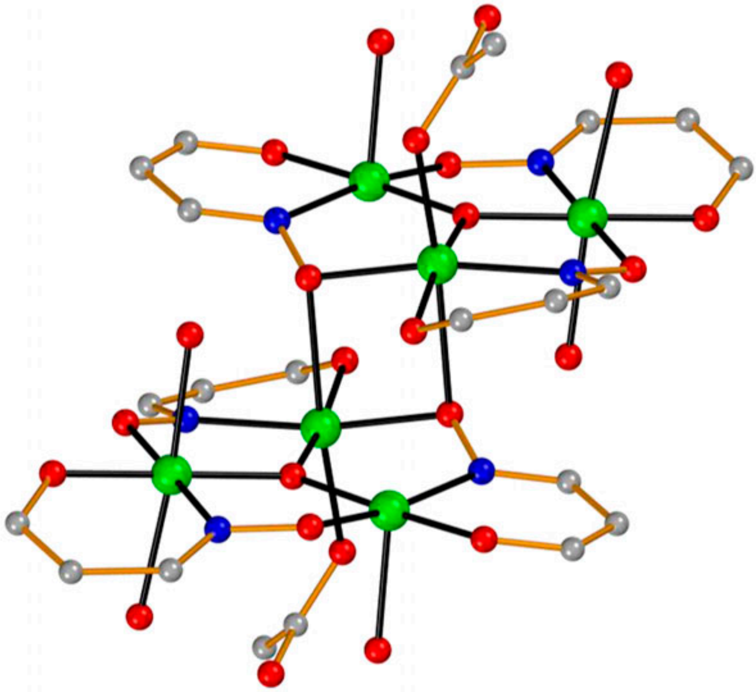

Figure 2. The $[Mn^{III}_6(\mu_3\text{-O})_2(\mu_3\text{-Rsao})_2(\mu_2\text{-Rsao})_4(RCO_2)_2(ROH)_6]$ core found in **2**. All hydrogens and several carbons and oxygens have been removed for clarity. Color code: Mn green, O red, N blue, C gray (see http://dx.doi.org/10.1080/00958972.2014.974583 for color version).

six alcohol molecules (MeOH or EtOH). As a consequence we recognize three different metal cores, shown in figure 1 (for **1**, **4**, and **5**), figure 2 (for **2**), and figure 3 (for **3**). All Mn^{III} ions display Jahn–Teller (JT) elongation with the carboxylate, the alcoholic, the bridging oximate, and the bridging phenolate O atoms occupying the axial positions (i.e. being on the JT axes). In this arrangement, the JT axes are approximately co-parallel, and perpendicular to the $[Mn_3]$ plane in each $[Mn_6]$. Each $[Mn^{III}{}_3(\mu_3\text{-}O)]^{7+}$ triangular unit is essentially equilateral, with the distances between Mn ions being within the 3.158–3.276 Å range. The central μ_3-O^{2-} ion deviates from the Mn_3 plane by 0.196 Å and 0.225 Å (in **1**), 0.082 Å and 0.093 Å (in **2**), 0.076 Å (in **3**), 0.226 Å (in **4**), and 0.178 Å (in **5**). The Mn–N–O–Mn torsion angles for **1** are 11.81°, 21.41°, and 37.42° (for $[Mn_6]_A$), 3.64°, 21.32°, and 28.24° (for $[Mn_6]_B$); for **2** are 19.69°, 20.84°, and 29.53° (for $[Mn_6]_A$), 17.38°, 23.43°, and 32.42°

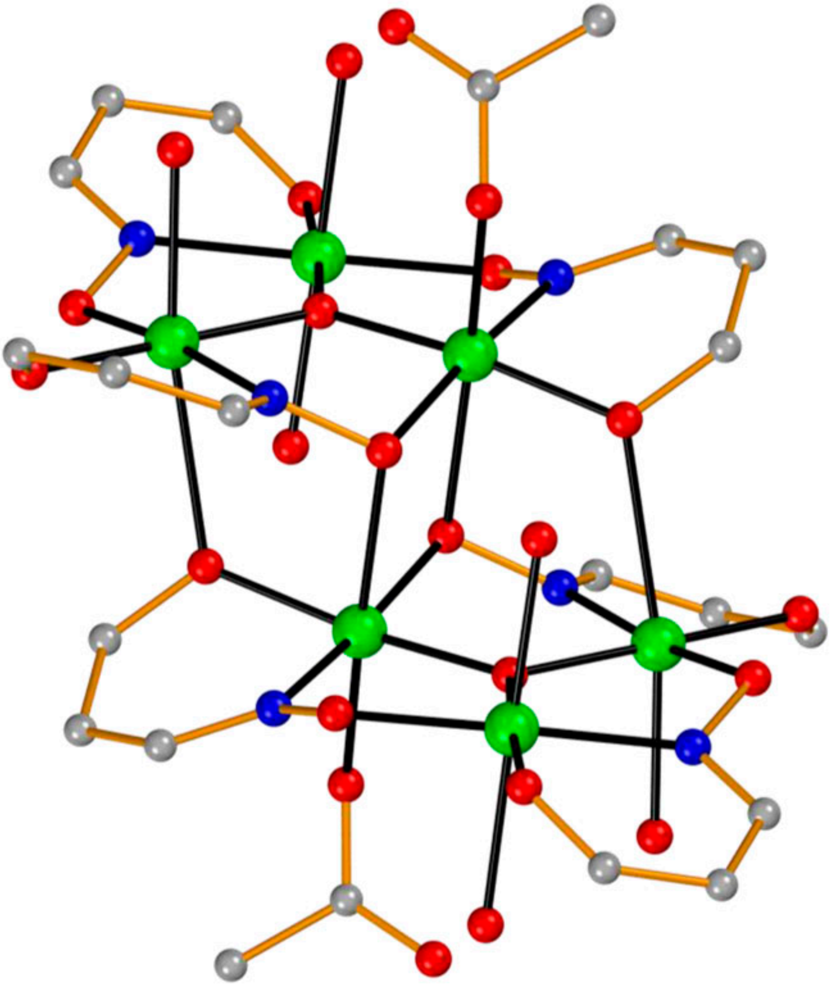

Figure 3. The $[Mn^{III}{}_6(\mu_3\text{-}O)_2(\mu_3\text{-}Rsao)_4(\mu_2\text{-}Rsao)_2(RCO_2)_2(ROH)_6]$ core found in **3**. All hydrogens and several carbons and oxygens have been removed for clarity. Color code: Mn green, O red, N blue, C gray (see http://dx.doi.org/10.1080/00958972.2014.974583 for color version).

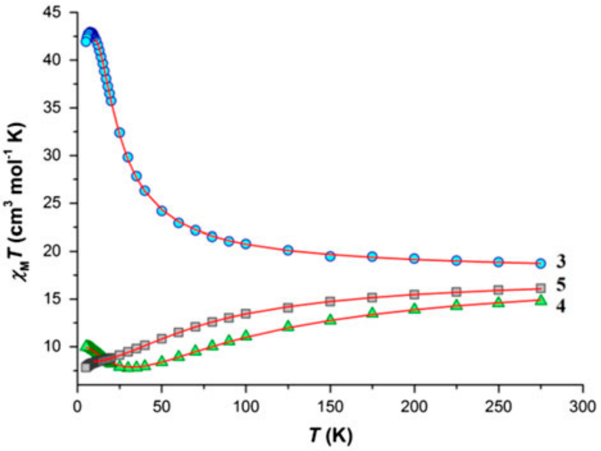

Figure 4. $\chi_M T$ *vs.* T plots for **3** (○), **4** (Δ), and **5** (□). The solid lines represent the best fit of the experimental data – see text for details.

(for $[Mn_6]_B$); for **3** are 31.39°, 31.64°, and 43.36°; for **4** are 3.81°, 18.62°, and 20.49° and for **5** are 8.18°, 22.57°, and 31.77°.

3.3. *Magnetic properties*

DC magnetic susceptibility studies were carried out on powdered crystalline samples of **3–5** from 5 to 275 K in a field of 0.1 T. The $\chi_M T$ *versus* T data for **3**, **4**, and **5** are plotted in figure 4. Complexes **1** and **2** were not measured since they comprise two crystallographically independent $[Mn_6]$ moieties in their unit cells. The $\chi_M T$ values for **4** and **5** at 275 K are 14.77 and 16.12 cm^3 K mol^{-1}, respectively, and are lower than the expected spin-only ($g = 2$) value for six non-interacting Mn^{III} centers of 18 cm^3 K mol^{-1}, suggesting the presence of dominant antiferromagnetic exchange. The $\chi_M T$ value for **3** at 275 K is 18.71 cm^3 K mol^{-1} and is higher than the expected spin-only value for six non-interacting Mn^{III} centers, suggesting the presence of dominant ferromagnetic exchange. The $\chi_M T$ value for **3** increases gradually as temperature is decreased until approximately 7.5 K reaching a value of 42.94 cm^3 K mol^{-1} and then decreases to a value of 41.92 cm^3 K mol^{-1} at 5 K. The $\chi_M T$ value for **4** decreases gradually as temperature is decreased until approximately 30 K reaching a value of 7.76 cm^3 K mol^{-1} and then increases to a value of 9.98 cm^3 K mol^{-1} at 5 K. The $\chi_M T$ value for **5** decreases gradually as temperature is decreased reaching a value of 7.81 cm^3 K mol^{-1} at 5 K.

$$\hat{H}_{ex} = -2J\left(\hat{S}_1\hat{S}_2 + \hat{S}_1\hat{S}_3 + \hat{S}_2\hat{S}_3 + \hat{S}_2\hat{S}_5 + \hat{S}_2\hat{S}_6 + \hat{S}_3\hat{S}_5 + \hat{S}_4\hat{S}_5 + \hat{S}_4\hat{S}_6 + \hat{S}_5\hat{S}_6\right) \quad (1)$$

$$\hat{H}_{ex} = -2J_1\left(\hat{S}_1\hat{S}_2 + \hat{S}_1\hat{S}_3 + \hat{S}_4\hat{S}_5 + \hat{S}_4\hat{S}_6\right) - 2J_2\left(\hat{S}_2\hat{S}_3 + \hat{S}_5\hat{S}_6\right) - 2J_3\left(\hat{S}_2\hat{S}_5 + \hat{S}_2\hat{S}_6 + \hat{S}_3\hat{S}_5\right) \quad (2)$$

$$\hat{H}_{ex} = -2J_1\left(\hat{S}_1\hat{S}_2 + \hat{S}_2\hat{S}_3 + \hat{S}_2\hat{S}_5 + \hat{S}_2\hat{S}_6 + \hat{S}_3\hat{S}_5 + \hat{S}_4\hat{S}_5 + \hat{S}_5\hat{S}_6\right) - 2J_2\left(\hat{S}_1\hat{S}_3 + \hat{S}_4\hat{S}_6\right) \quad (3)$$

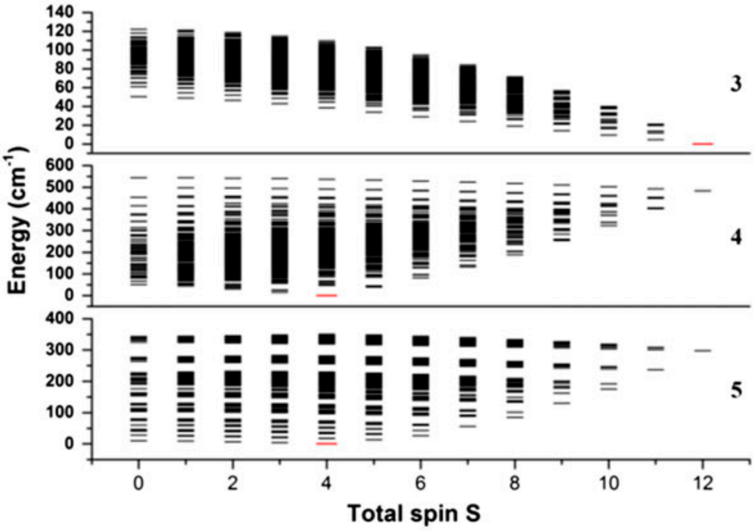

Figure 5. Plot of energy *vs.* total spin (S) state for **3**–**5**. The ground state for **3** is an $S = 12$ state and for **4** and **5**, an $S = 4$ state. In each case a band of low-lying excited states lies in close proximity to the ground state.

Considering the structural data and the number of significantly different Mn–N–O–Mn torsion angles within the [Mn_3] units of each [Mn_6] a 1-*J*, a 3-*J,* and a 2-*J* model (scheme 2) were utilized to fit the experimental data for **3**, **4**, and **5**, respectively. The experimental data were satisfactorily fitted using the program PHI [76] and employing the spin Hamiltonian in equations (1)–(3) for **3**, **4**, and **5**, respectively. The best fits (red lines in figure 4) gave the following parameters for **3** (down to 10 K), **4** and **5** (down to 10 K), respectively: $g = 1.98$, $J = +0.98$ cm^{-1}, and $zJ = -0.02$ cm^{-1}; $g = 2.00$ (fixed), $J_1 = -6.79$ cm^{-1}, $J_2 = -1.41$ cm^{-1}, and $J_3 = +1.17$ cm^{-1}; $g = 1.98$, $J_1 = +0.50$ cm^{-1}, and $J_2 = -8.02$ cm^{-1} (where zJ describes the intermolecular interactions in a mean field approximation), figure 5. For **3** this results in a spin ground state $S = 12$, with the first excited state ($S = 11$) located ~4.7 cm^{-1} above the ground state; for **4** and **5** the spin ground state is $S = 4$, with the first excited state ($S = 3$) located ~15 cm^{-1} and ~4 cm^{-1}, respectively, above the ground state (figure 5).

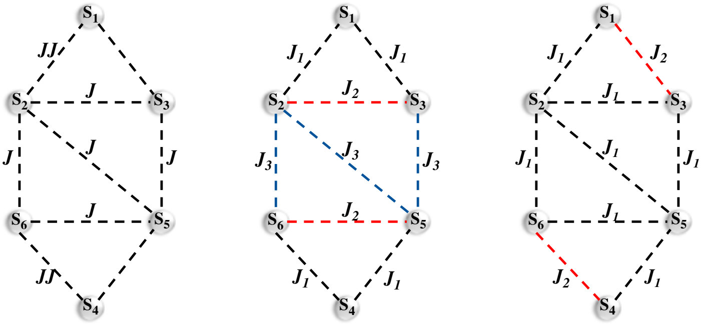

Complex **3** Complex **4** Complex **5**

Scheme 2. Schematic detailing the models employed to fit the experimental data for **3**, **4**, and **5**, respectively.

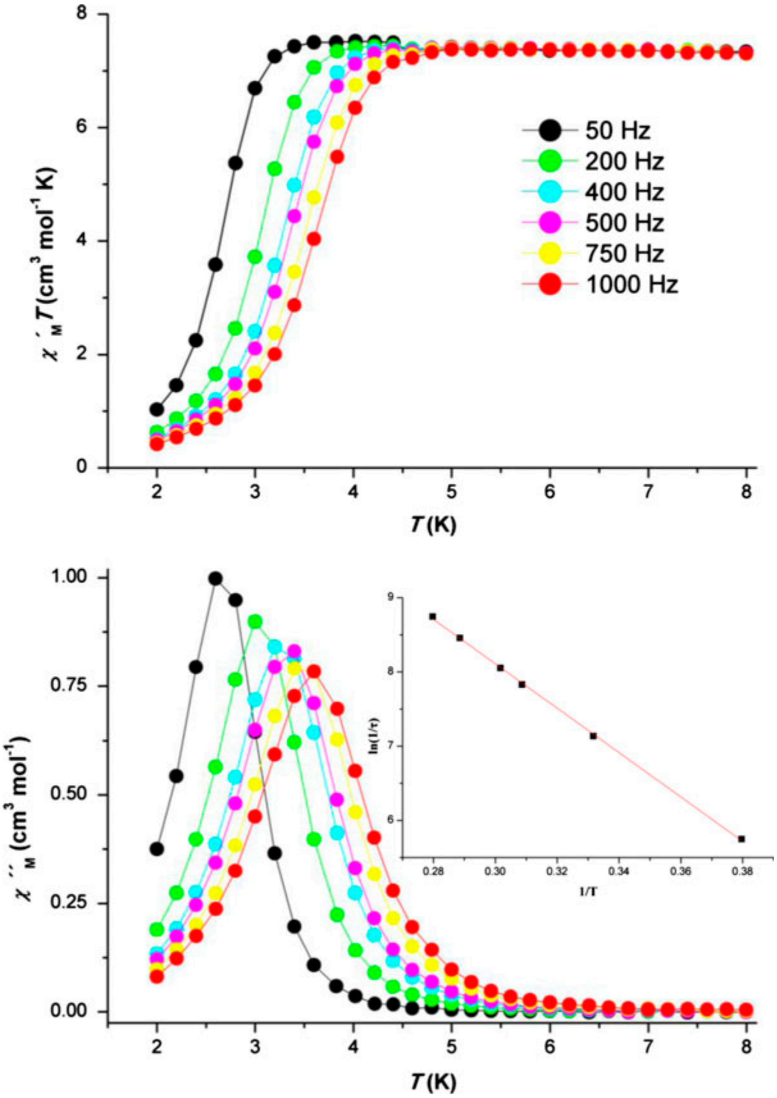

Figure 6. Plots of χ_M' (top) and χ_M'' (bottom) *vs.* T for **4** at the indicated temperature and frequency ranges. Inset: Arrhenius plot constructed from the χ_M'' data to afford $\tau_0 = 3.82 \times 10^{-8}$ s and $U_{\mathrm{eff}} = 30$ K.

Magnetization data were collected from 0.5 to 7 T and 2.0–7.0 K to further determine the nature of the spin ground state for the complexes. The plots of the magnetization ($M/N\mu_B$) *versus* applied field (H) for **3**, **4**, and **5** are shown in figures S1–S3 (see online supplemental material at http://dx.doi.org/10.1080/00958972.2014.974583). The data could not be successfully fitted using a simple model that assumes only population of the ground state, as expected from the analysis of the DC data above. The reason, as with most members of this family [15], is the presence of multiple low-lying excited states resulting from the weak intramolecular exchange. In the weak exchange limit ($J \approx d_{\mathrm{ion}}$), the Giant Spin Approximation breaks down and a more detailed multi-spin Hamiltonian approach, as reported previously [15, 77–79], is required. Such an analysis, however, is beyond the scope of the current paper.

AC susceptibility measurements are performed in the 2–8 K range in zero applied DC field and a 3.5 G AC field oscillating at 50–1000 Hz for **3** (figure S4), **4** (figure 6), and **5** (figure S5). A cusp in the real component χ_M' is accompanied by a non-zero imaginary component χ_M'' at ~6 K for **3** and ~4 K for **4** and **5**. The maxima for all complexes are strongly frequency dependent, suggesting super-paramagnetic blocking of the magnetization. Arrhenius plots (inset in figure 6 for **4**) constructed from the χ_M'' data afforded $\tau_0 = 2.52 \times 10^{-11}$ s and $U_{\text{eff}} = 74$ K (51.40 cm^{-1}) for **3**, $\tau_0 = 3.82 \times 10^{-8}$ s and $U_{\text{eff}} = 30$ K (20.77 cm^{-1}) for **4**, and $\tau_0 = 1.44 \times 10^{-8}$ s and $U_{\text{eff}} = 28$ K (19.19 cm^{-1}) for **5**, consistent with that observed for structurally analogous family members.

4. Conclusion

Our adventures in employing salicylic acid, 2,6-dihydroxy benzoic acid, and naphthalene-1,8-dicarboxylic acid in Mn(III) salicylaldoximate chemistry have afforded a family of five hexanuclear clusters that are similar to the many $[\text{Mn}_6]$s obtained so far – single-crystal X-ray crystallography revealing three different metal cores for the five complexes. Magnetic characterization for **3**, **4**, and **5** indicated spin ground states of $S = 12$ for **3** and $S = 4$ for **4** and **5**. Frequency dependent AC susceptibility signals suggest super-paramagnetic blocking of the magnetization for all complexes with U_{eff} values of 73.98 K (**3**), 29.9 K (**4**), and 27.63 K (**5**).

Supplementary material

CIF files of complexes **1–5** and figures.

Acknowledgements

This research has been co-financed by the European Union (European Social Fund – ESF) and Greek national funds through the Operational Program “Education and Lifelong Learning” of the National Strategic Reference Framework (NSRF) – Research Funding Program: THALES. Investing in knowledge society through the European Social Fund.
The Special Account for Research Grants (SARG) of the National and Kapodistrian University of Athens and the Bodossaki Foundation are gratefully acknowledge for partial support of this work. EKB and RI thank the EPSRC and Royal Society of Edinburgh for funding.

References

[1] P. Chaudhuri, M. Hess, E. Rentschler, T. Weyhermüller, U. Flörke. *New J. Chem.*, **22**, 553 (1998).
[2] C.J. Milios, C.P. Raptopoulou, A. Terzis, F. Lloret, R. Vicente, S.P. Perlepes, A. Escuer. *Angew. Chem. Int. Ed.*, **43**, 210 (2004).

[3] C.J. Milios, A. Vinslava, A.G. Whittaker, S. Parsons, W. Wernsdorfer, G. Christou, S.P. Perlepes, E.K. Brechin. *Inorg. Chem.*, **45**, 5272 (2006).

[4] C.J. Milios, R. Inglis, R. Bagai, W. Wernsdorfer, A. Collins, S. Moggach, S. Parsons, S.P. Perlepes, G. Christou, E.K. Brechin. *Chem. Commun.*, 3476 (2007).

[5] C.J. Milios, R. Inglis, A. Vinslava, R. Bagai, W. Wernsdorfer, S. Parsons, S.P. Perlepes, G. Christou, E.K. Brechin. *J. Am. Chem. Soc.*, **129**, 12505 (2007).

[6] C.J. Milios, A. Vinslava, W. Wernsdorfer, S. Moggach, S. Parsons, S.P. Perlepes, G. Christou, E.K. Brechin. *J. Am. Chem. Soc.*, **129**, 2754 (2007).

[7] C.J. Milios, A. Vinslava, W. Wernsdorfer, A. Prescimone, P.A. Wood, S. Parsons, S.P. Perlepes, G. Christou, E.K. Brechin. *J. Am. Chem. Soc.*, **129**, 6547 (2007).

[8] C.J. Milios, A. Vinslava, P.A. Wood, S. Parsons, W. Wernsdorfer, G. Christou, S.P. Perlepes, E.K. Brechin. *J. Am. Chem. Soc.*, **129**, 8 (2007).

[9] L.F. Jones, M.E. Cochrane, B.D. Koivisto, D.A. Leigh, S.P. Perlepes, W. Wernsdorfer, E.K. Brechin. *Inorg. Chim. Acta*, **361**, 3420 (2008).

[10] L.F. Jones, R. Inglis, M.E. Cochrane, K. Mason, A. Collins, S. Parsons, S.P. Perlepes, E.K. Brechin. *Dalton Trans.*, 6205 (2008).

[11] L.F. Jones, C.J. Milios, A. Prescimone, M. Evangelisti, E.K. Brechin. *C.R. Chim.*, **11**, 1175 (2008).

[12] F. Moro, V. Corradini, M. Evangelisti, V. De Renzi, R. Biagi, U. del Pennino, C.J. Milios, L.F. Jones, E.K. Brechin. *J. Phys. Chem. B*, **112**, 9729 (2008).

[13] A. Prescimone, C.J. Milios, S. Moggach, J.E. Warren, A.R. Lennie, J. Sanchez-Benitez, K. Kamenev, R. Bircher, M. Murrie, S. Parsons, E.K. Brechin. *Angew. Chem. Int. Ed.*, **47**, 2828 (2008).

[14] C.P. Raptopoulou, A.K. Boudalis, K.N. Lazarou, V. Psycharis, N. Panopoulos, M. Fardis, G. Diamantopoulos, J.-P. Tuchagues, A. Mari, G. Papavassiliou. *Polyhedron*, **27**, 3575 (2008).

[15] R. Inglis, L.F. Jones, C.J. Milios, S. Datta, A. Collins, S. Parsons, W. Wernsdorfer, S. Hill, S.P. Perlepes, S. Piligkos, E.K. Brechin. *Dalton Trans.*, 3403 (2009).

[16] A. Prescimone, C.J. Milios, J. Sanchez-Benitez, K.V. Kamenev, C. Loose, J. Kortus, S. Moggach, M. Murrie, J.E. Warren, A.R. Lennie, S. Parsons, E.K. Brechin. *Dalton Trans.*, 4858 (2009).

[17] C.-I. Yang, K.-H. Cheng, M. Nakano, G.-H. Lee, H.-L. Tsai. *Polyhedron*, **28**, 1842 (2009).

[18] R. Inglis, S.J. Dalgarno, E.K. Brechin. *Dalton Trans.*, **39**, 4826 (2010).

[19] X. Song, R. Liu, S. Zhang, L. Li. *Inorg. Chem. Commun.*, **13**, 828 (2010).

[20] A.R. Tomsa, J. Martínez-Lillo, Y. Li, L.M. Chamoreau, K. Boubekeur, F. Farias, M.A. Novak, E. Cremades, E. Ruiz, A. Proust, M. Verdaguer, P. Gouzerh. *Chem. Commun.*, **46**, 5106 (2010).

[21] G.-Y. An, A.-L. Cui, H.-Z. Kou. *Inorg. Chem. Commun.*, **14**, 1475 (2011).

[22] V. Kotzabasaki, R. Inglis, M. Siczek, T. Lis, E.K. Brechin, C.J. Milios. *Dalton Trans.*, **40**, 1693 (2011).

[23] C.-L. Zhou, Z.-M. Wang, B.-W. Wang, S. Gao. *Polyhedron*, **30**, 3279 (2011).

[24] M. Hołyńska, S. Dehnen. *Z. Anorg. Allg. Chem.*, **638**, 763 (2012).

[25] X.-T. Liu, J.-X. Li, X. Fei, Q.-L. Wu, B. Yang. *Chin. J. Inorg. Chem.*, **28**, 1234 (2012).

[26] J. Martínez-Lillo, L.-M. Chamoreau, A. Proust, M. Verdaguer, P. Gouzerh. *C.R. Chim.*, **15**, 889 (2012).

[27] J. Martínez-Lillo, A.R. Tomsa, Y. Li, L.M. Chamoreau, E. Cremades, E. Ruiz, A.L. Barra, A. Proust, M. Verdaguer, P. Gouzerh. *Dalton Trans.*, **41**, 13668 (2012).

[28] G. Novitchi, G. Pilet, D. Luneau. *C.R. Chim.*, **15**, 937 (2012).

[29] J. Martínez-Lillo, N. Dolan, E.K. Brechin. *Dalton Trans.*, **42**, 12824 (2013).

[30] C.J. Milios, P.A. Wood, S. Parsons, D. Foguet-Albiol, C. Lampropoulos, G. Christou, S.P. Perlepes, E.K. Brechin. *Inorg. Chim. Acta*, **360**, 3932 (2007).

[31] H.B. Xu, B.W. Wang, F. Pan, Z.M. Wang, S. Gao. *Angew. Chem. Int. Ed.*, **46**, 7388 (2007).

[32] R. Inglis, L.F. Jones, G. Karotsis, A. Collins, S. Parsons, S.P. Perlepes, W. Wernsdorfer, E.K. Brechin. *Chem. Commun.*, 5924 (2008).

[33] R. Inglis, L.F. Jones, K. Mason, A. Collins, S.A. Moggach, S. Parsons, S.P. Perlepes, W. Wernsdorfer, E.K. Brechin. *Chem. Eur. J.*, **14**, 9117 (2008).

[34] C.I. Yang, W. Wernsdorfer, K.H. Cheng, M. Nakano, G.H. Lee, H.L. Tsai. *Inorg. Chem.*, **47**, 10184 (2008).

[35] R. Inglis, G.S. Papaefstathiou, W. Wernsdorfer, E.K. Brechin. *Aust. J. Chem.*, **62**, 1108 (2009).

[36] C.J. Milios, R. Inglis, L.F. Jones, A. Prescimone, S. Parsons, W. Wernsdorfer, E.K. Brechin. *Dalton Trans.*, 2812 (2009).

[37] C.C. Stoumpos, R. Inglis, G. Karotsis, L.F. Jones, A. Collins, S. Parsons, C.J. Milios, G.S. Papaefstathiou, E.K. Brechin. *Cryst. Growth Des.*, **9**, 24 (2009).

[38] C. Kozoni, E. Manolopoulou, M. Siczek, T. Lis, E.K. Brechin, C.J. Milios. *Dalton Trans*, **39**, 7943 (2010).

[39] E. Manolopoulou, C.C. Stoumpos, M. Siczek, T. Lis, E.K. Brechin, C.J. Milios. *Eur. J. Inorg. Chem.*, **2010**, 483 (2010).

[40] C.-I. Yang, K.-H. Cheng, S.-P. Hung, M. Nakano, H.-L. Tsai. *Polyhedron*, **30**, 3272 (2011).

[41] C.-I. Yang, P.-Y. Feng, Y.-T. Chen, Y.-J. Tsai, G.-H. Lee, H.-L. Tsai. *Polyhedron*, **30**, 3265 (2011).

[42] M. Hołyńska, N. Frank, S. Dehnen. *Z. Anorg. Allg. Chem.*, **638**, 2248 (2012).

[43] L.-L. Li, S.-N. Wang, J. Lu, F.A.N. Cao, L.-Q. Kong, J.-M. Dou, D.-C. Li. *J. Coord. Chem.*, **66**, 306 (2013).

[44] W.-K. Dong, C.-Y. Zhao, Y.-X. Sun, X.-L. Tang, X.-N. He. *Inorg. Chem. Commun.*, **12**, 234 (2009).

[45] L.F. Jones, A. Prescimone, M. Evangelisti, E.K. Brechin. *Chem. Commun.*, 2023 (2009).

[46] M. Haryono, M. Kalisz, R. Sibille, R. Lescouëzec, C. Fave, G. Trippe-Allard, Y. Li, M. Seuleiman, H. Rousselière, A.M. Balkhy, J.-C. Lacroix, Y. Journaux. *Dalton Trans.*, **39**, 4751 (2010).

[47] P.L. Feng, C.J. Stephenson, D.N. Hendrickson. *Inorg. Chem.*, **49**, 6393 (2010).

[48] R. Inglis, A.D. Katsenis, A. Collins, F. White, C.J. Milios, G.S. Papaefstathiou, E.K. Brechin. *CrystEngComm*, **12**, 2064 (2010).

[49] X. Song, P. Yang, X. Mei, L. Li, D. Liao. *Eur. J. Inorg. Chem.*, 1689 (2010).

[50] C.-I. Yang, S.-P. Hung, G.-H. Lee, M. Nakano, H.-L. Tsai. *Inorg. Chem.*, **49**, 7617 (2010).

[51] C.-I. Yang, Y.-J. Tsai, S.-P. Hung, H.-L. Tsai, M. Nakano. *Chem. Commun.*, **46**, 5716 (2010).

[52] J.-P. Geng, Z.-X. Wang, X. He, H.-P. Xiao, M.-X. Li. *Inorg. Chem. Commun.*, **14**, 997 (2011).

[53] V. Kotzabasaki, M. Siczek, T. Lis, C.J. Milios. *Inorg. Chem. Commun.*, **14**, 213 (2011).

[54] H.-L. Tsai, C.-I. Yang, W. Wernsdorfer, S.-H. Huang, S.-Y. Jhan, M.-H. Liu, G.-H. Lee. *Inorg. Chem.*, **51**, 13171 (2012).

[55] K.N. Lazarou, Y. Sanakis, A.K. Boudalis, M. Pissas, V. Psycharis, C.P. Raptopoulou. *Polyhedron*, **52**, 917 (2013).

[56] M. Manoli, R. Inglis, M.J. Manos, G.S. Papaefstathiou, E.K. Brechin, A.J. Tasiopoulos. *Chem. Commun.*, **49**, 1061 (2013).

[57] T. Shiga, K. Maruyama, G.N. Newton, R. Inglis, E.K. Brechin, H. Oshio. *Inorg. Chem.*, **53**, 4272 (2014).

[58] A.D. Katsenis, R. Inglis, A. Prescimone, E.K. Brechin, G.S. Papaefstathiou. *CrystEngComm*, **14**, 1216 (2012).

[59] (a) C.J. Milios, A. Prescimone, A. Mishra, S. Parsons, W. Wernsdorfer, G. Christou, S.P. Perlepes, E.K. Brechin. *Chem. Commun.*, 153 (2007). (b) R. Inglis, C.C. Stoumpos, A. Prescimone, M. Siczek, T. Lis, W. Wernsdorfer, E.K. Brechin, C.J. Milios. *Dalton Trans.*, **39**, 4777 (2010).

[60] (a) A.S. Kumbhar, M.P. Mulay, S.B. Padhye, S.S. Tavale, V.G. Puranik. *Struct. Chem.*, **19**, 735 (2008). (b) M. Hołyńska, C. Pietzonka, S. Dehnen. *Z. Anorg. Allg. Chem.*, **637**, 556 (2011).

[61] P.L. Feng, C.J. Stephenson, A. Amjad, G. Ogawa, E. del Barco, D.N. Hendrickson. *Inorg. Chem.*, **49**, 1304 (2010).

[62] C.J. Milios, I.A. Gass, A. Vinslava, L. Budd, S. Parsons, W. Wernsdorfer, S.P. Perlepes, G. Christou, E.K. Brechin. *Inorg. Chem.*, **46**, 6215 (2007).

[63] C.J. Milios, R. Inglis, A. Vinslava, A. Prescimone, S. Parsons, S.P. Perlepes, G. Christou, E.K. Brechin. *Chem. Commun.*, 2738 (2007).

[64] R. Inglis, F. White, S. Piligkos, W. Wernsdorfer, E.K. Brechin, G.S. Papaefstathiou. *Chem. Commun.*, **47**, 3090 (2011).

[65] S. Wang, L. Kong, H. Yang, Z. He, Z. Jiang, D. Li, S. Zeng, M. Niu, Y. Song, J. Dou. *Inorg. Chem.*, **50**, 2705 (2011).

[66] M. Hołyńska, N. Frank, C. Pichon, I.-R. Jeon, R. Clérac, S. Dehnen. *Inorg. Chem.*, **52**, 7317 (2013).

[67] B. Cordero, O. Roubeau, S.J. Teat, A. Escuer. *Dalton Trans.*, **40**, 7127 (2011).

[68] M.-H. Liu, C.-I. Yang, G.-H. Lee, H.-L. Tsai. *Inorg. Chem. Commun.*, **14**, 1136 (2011).

[69] M. Hołyńska, R. Clérac, S. Dehnen. *Eur. J. Inorg. Chem.*, **33**, 5500 (2012).

[70] M. Manoli, R. Inglis, M.J. Manos, V. Nastopoulos, W. Wernsdorfer, E.K. Brechin, A.J. Tasiopoulos. *Angew. Chem. Int. Ed.*, **50**, 4441 (2011).

[71] C. Birnara, V.G. Kessler, G.S. Papaefstathiou. *Polyhedron*, **28**, 3291 (2009).

[72] M.C. Burla, R. Caliandro, M. Camalli, B. Carrozzini, G.L. Cascarano, L. De Caro, C. Giacovazzo, G. Polidori, R. Spagna. *J. Appl. Crystallogr.*, **38**, 381 (2005).

[73] A. Altomare, M.C. Burla, M. Camalli, G.L. Cascarano, C. Giacovazzo, A. Guagliardi, A.G.G. Moliterni, G. Polidori, R. Spagna. *J. Appl. Crystallogr.*, **32**, 115 (1999).

[74] G.M. Sheldrick. *SHELXS-97, Program for the Solution of Crystal Structures*, University of Göttingen, Göttingen (1997).

[75] G.M. Sheldrick. *SHELXL-97, Program for X-ray Crystal Structure Refinement*, University of Göttingen, Göttingen (1997).

[76] N.F. Chilton, R.P. Anderson, L.D. Turner, A. Soncini, K.S. Murray. *J. Comput. Chem.*, **34**, 1164 (2013).

[77] S. Carretta, T. Guidi, P. Santini, G. Amoretti, O. Pieper, B. Lake, J. van Slageren, F. Hallak, W. Wernsdorfer, H. Mutka, M. Russina, C. Milios, E. Brechin. *Phys. Rev. Lett.*, **100**, 157203 (2008).

[78] P.L. Feng, C. Koo, J.J. Henderson, P. Manning, M. Nakano, E. del Barco, S. Hill, D.N. Hendrickson. *Inorg. Chem.*, **48**, 3480 (2009).

[79] O. Pieper, T. Guidi, S. Carretta, J. van Slageren, F. El Hallak, B. Lake, P. Santini, G. Amoretti, H. Mutka, M. Koza, M. Russina, A. Schnegg, C.J. Milios, E.K. Brechin, A. Julià, J. Tejada. *Phys. Rev. B*, **81**, 174420 (2010).